



Supplement of

Asian dust transport of proteinaceous matter from the Gobi Desert to northern China

Ren-Guo Zhu et al.

Correspondence to: Hua-Yun Xiao (xiaohuayun@sjtu.edu.cn)

The copyright of individual parts of the supplement might differ from the article licence.

Contents of this file

Section S1~S2

Table S1~S5

Figure S1~S5

Introduction

The supporting information contains the supplementary Section S1~S2, Table S1~S5 and Figure S1~S5.

Section S1. Uncertainty of protein-N deposition fluxes

The atmospheric deposition fluxes of CAAs ($\text{mg N m}^{-2} \text{d}^{-1}$) at four sampling sites are estimated from equation (S1):

$$F_{dry} = C \cdot V_d \quad (\text{S1})$$

The uncertainty range of protein-N deposition fluxes can be calculated by using the formula (S2) for error propagation for multiplication:

$$\left(\frac{\Delta F_{dry}}{F_{dry}}\right)^2 = \left(\frac{\Delta C}{C}\right)^2 + \left(\frac{\Delta V_d}{V_d}\right)^2 \quad (\text{S2})$$

The uncertainty for the deposition velocity of aerosol protein-N in this study was set to a factor of 3. The concentration C is measured with negligible uncertainty (0.1) compared to V_d , the term $\Delta C/C$ can be considered zero. Therefore, the equation simplifies to:

$$\frac{\Delta F_{dry}}{F_{dry}} = \frac{\Delta V_d}{V_d} \quad (\text{S3})$$

Given $\Delta V_d/V_d = 3$:

$$\frac{\Delta F_{dry}}{F_{dry}} = 3$$

Consequently, F_{dry} will also have the same factor of uncertainty:

$$F_{dry, min} = C \cdot \frac{V_d}{3}$$
$$F_{dry, max} = C \cdot 3 \cdot V_d$$

Each deposition fluxes of protein-N with the uncertainty range at the four sampling cities was provided in Figure 8.

Section S2. Stable Isotope Analysis in R

The Bayesian mixing models in R model (MixSIAR) has been widely used to determine diet composition, population structure, and animal movement, because it can use the isotope values (biotracer data) to estimate the proportions of source contributions to a mixture, and incorporate the uncertainties associated with source isotope values (Stock and Semmens, 2016, Song et al., 2021). In our study, the MixSIAR model with $\delta^{15}\text{N}$ values of both glycine and leucine was used to incorporate source apportionment of CAAs in Taiyuan during the non-dust period and dust period, respectively. Quantifying dust source contributions using nitrogen isotopic values from single amino acids (e.g., exclusively glycine or leucine) may introduce substantial uncertainty. This limitation stems from the fact that $\delta^{15}\text{N}$ values of glycine or leucine in Gobi dust show no statistically significant differences compared to those of urban road soils across all study sites ($p > 0.05$; Figure S5). Therefore, both $\delta^{15}\text{N}$ values of both glycine and leucine from local and the Gobi dust sources were used to minimal uncertainty. Details on the assumed values for each potential end-member are of great importance. As discussed in section 4.1, local dominant plants, surface road dust and anthropogenic industrial activities were the major sources of CAAs in $\text{PM}_{2.5}$ during the non-dust period. Therefore, three major sources, including local dominant plants, surface road dust and anthropogenic sources were used to simulate the relative contributions of major urban protein sources during non-dust periods in Taiyuan (Table S1). Four distinct source categories were used to calculate their respective contribution to urban proteinaceous matter in $\text{PM}_{2.5}$: dust from Gobi Desert, local dominant plants, road dust and anthropogenic activity sources in Taiyuan. In our estimations, uncertainties associated in the source analysis were derived from the $\delta^{15}\text{N}$ variabilities of major combined Gly and Leu sources (mean \pm SD $\delta^{15}\text{N}$ values of each source were input; Table S1). The result of MixSIAR model was exhibited in Table S5.

Table S1. Information on the sampling sites and numbers, average and standard deviation of Ala%/Pro%, Gly%/Pro%, Glu%/Pro%, $\delta^{15}\text{N}$ values of combined glycine and combined leucine determined in these samples.

Location	Latitude ($^{\circ}\text{N}$) and longitude ($^{\circ}\text{E}$)	Samples	number	Ala%/Pro%	Gly%/Pro%	Glu%/Pro%	$\delta^{15}\text{N}$ values of combined glycine	$\delta^{15}\text{N}$ values of combined leucine
Soil								
Gobi Desert	43.46~43.60, 112.00~112.05	Surface soil	n=5	2.0 \pm 0.4	1.8 \pm 0.5	0.1 \pm 0.1	2.7 \pm 0.4	1.9 \pm 1.8
Beijing	39.98, 116.31	Surface soil	n=6	1.6 \pm 0.3	1.8 \pm 0.6	1.1 \pm 0.4	1.7 \pm 0.4	3.0 \pm 1.4
Tianjin	39.11, 117.17	Surface soil	n=4	1.3 \pm 0.3	1.1 \pm 0.2	0.8 \pm 0.5	0.6 \pm 0.6	-0.6 \pm 1.1
Shijiazhuang	38.03, 114.51	Surface soil	n=3	0.8 \pm 0.2	0.6 \pm 0.2	0.8 \pm 0.3	1.6 \pm 0.2	2.9 \pm 0.5
Taiyuan	37.86, 112.51	Surface soil	n=5	1.1 \pm 0.2	1.0 \pm 0.2	0.8 \pm 0.2	4.2 \pm 2.1	3.3 \pm 0.8
Plant								
Gobi Desert	43.46~43.60, 112.00~112.05	<i>Chenopodium ambrosioides</i>	n=3	0.5 \pm 0.4	0.2 \pm 0.4	2.7 \pm 0.8	8.3 \pm 0.4	16.1 \pm 1.4
Gobi Desert	43.59, 112.04	<i>Tripogon chinensis</i>	n=4	2.0 \pm 0.8	0.3 \pm 0.4	6.1 \pm 0.5	10.8 \pm 0.2	11.0 \pm 0.8
Gobi Desert	43.59, 112.04	<i>Tamarix chinensis</i>	n=5	2.7 \pm 0.9	0.7 \pm 0.6	65.6 \pm 3.5	6.8 \pm 0.7	8.9 \pm 1.7
Beijing	39.98, 116.31	<i>Platanus orientalis</i>	n=5	1.0 \pm 0.1	1.0 \pm 0.2	0.9 \pm 0.04	-8.7 \pm 0.6	-1.7 \pm 0.5
Tianjin	39.11, 117.17	<i>Platanus orientalis</i>	n=16	0.9 \pm 0.2	1.0 \pm 0.2	1.5 \pm 0.7	1.6 \pm 1.2	-0.8 \pm 1.0
Shijiazhuang	38.03, 114.51	<i>Platanus orientalis</i>	n=6	0.8 \pm 0.1	0.9 \pm 0.1	1.0 \pm 0.1	-6.9 \pm 0.4	-0.2 \pm 1.2
Taiyuan	37.86, 112.51	<i>Platanus orientalis</i>	n=5	0.6 \pm 0.04	0.7 \pm 0.05	0.9 \pm 0.2	-8.4 \pm 1.5	-2.2 \pm 1.6

Table S2. The recoveries and precision of CAA analysis.

Amino acids	Recovery (%)	Precision (%)
Glycine (Gly)	106.5	1.1
Alanine (Ala)	92.6	3.6
Aspartic acid (Asp)	95.0	8.6
Glutamic acid (Glu)	105.6	8.8
γ -amino butyric acid (Gaba)	95.7	7.7
Serine (Ser)	92.7	5.7
Proline (Pro)	93.2	6.7
Threonine (Thr)	90.0	6.1
Valine (Val)	95.5	1.3
Lysine (Lys)	82.5	6
Leucine (Leu)	92.0	0.8
Isoleucine (Ile)	93.1	2
Arginine (Arg)	85.4	9.4
Phenylalanine (Phe)	93.7	5.4
Ornithine (Orn)	91.5	9.9
Tyrosine (Tyr)	80.7	0.3
Histidine (His)	95.1	1.7
Methionine (Met)	86.6	2.7

Table S3. Particle Mass Concentrations and mean ratio of PM_{2.5} to PM₁₀ at four sampling sites. Please note BJ represent Beijing, TJ represent Tianjin, SJZ represent Shijiazhuang, TY represent Taiyuan.

Sampling sites	PM ₁₀ *		PM _{2.5} *		PM _{2.5} /PM ₁₀	
	dust	Non-dust	dust	Non-dust	dust	Non-dust
BJ	1224**	141	147**	93	0.1	0.7
TJ	849**	135	75	77	0.1	0.6
SJZ	761**	161	130**	63	0.2	0.4
TY	611**	189	122**	64	0.2	0.4

* Units are $\mu\text{g m}^{-3}$ for particle mass.

** $p < 0.01$

Table S4. Pearson correlations of the total concentration of the combined amino acids (TCAA) with the concentration of PM₁₀, NO₂, SO₂, O₃, as well as local meteorological conditions (including wind speed (WD), temperature (T) and relative humidity (RH)) in local cities.

		TCAA	PM ₁₀	WD	T	RH	NO ₂	SO ₂	O ₃
TCAA	r	1.00	0.82*	0.12	-0.15	-0.34	-0.29	-0.32	-0.30
	p value	--	0.00	0.56	0.45	0.08	0.15	0.11	0.13

Table S5. The mean, SD, and quantiles for each emission source proportion of the overall CAAs in PM_{2.5} during the dust and non-dust period in Taiyuan.

		Dust period								
		Mean	SD	2.50%	5%	25%	50%	75%	95%	97.50%
p. TY.	anthropogenic activities	0.359	0.1	0.172	0.208	0.292	0.352	0.421	0.536	0.576
	p.TY. Gobi dust	0.187	0.141	0.005	0.012	0.069	0.158	0.282	0.452	0.512
	p.TY.plant	0.126	0.103	0.005	0.009	0.046	0.098	0.187	0.333	0.387
	p.TY. road dust	0.327	0.198	0.012	0.024	0.163	0.323	0.481	0.662	0.708
		Non-dust period								
p.TY.	anthropogenic activities	0.458	0.122	0.252	0.278	0.374	0.444	0.535	0.679	0.714
	p.TJ.plant	0.016	0.026	0	0	0	0.005	0.021	0.072	0.094
	p.TY. road dust	0.462	0.209	0	0.008	0.369	0.523	0.609	0.713	0.739

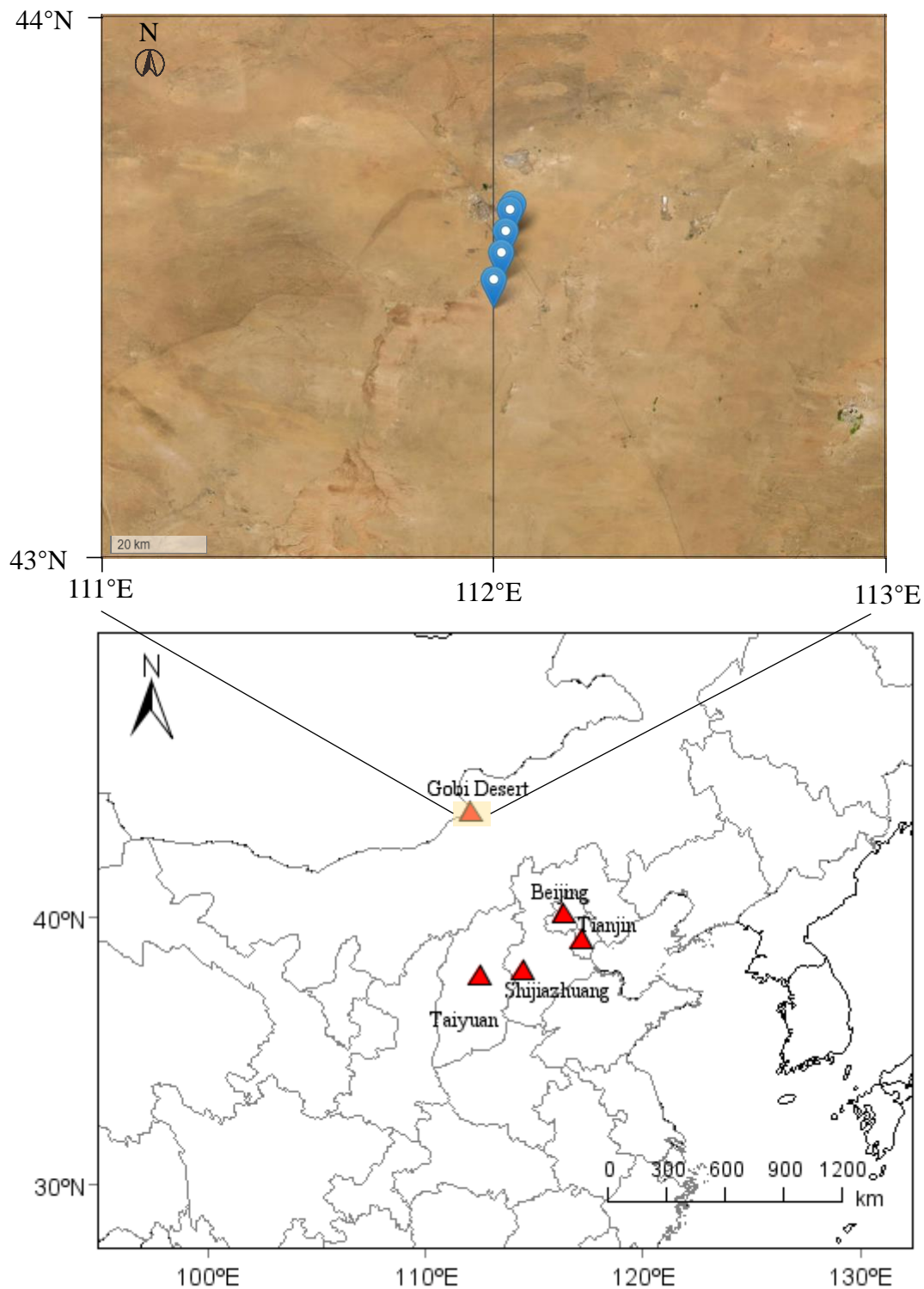


Figure S1. Sampling sites of the source region (Gobi Desert) and four urban areas in the downwind North China Plain, including Beijing, Tianjin, Shijiazhuang and Taiyuan. Data source: NASA Worldview (<https://worldview.earthdata.nasa.gov>), accessed on 7 Feb 2025.

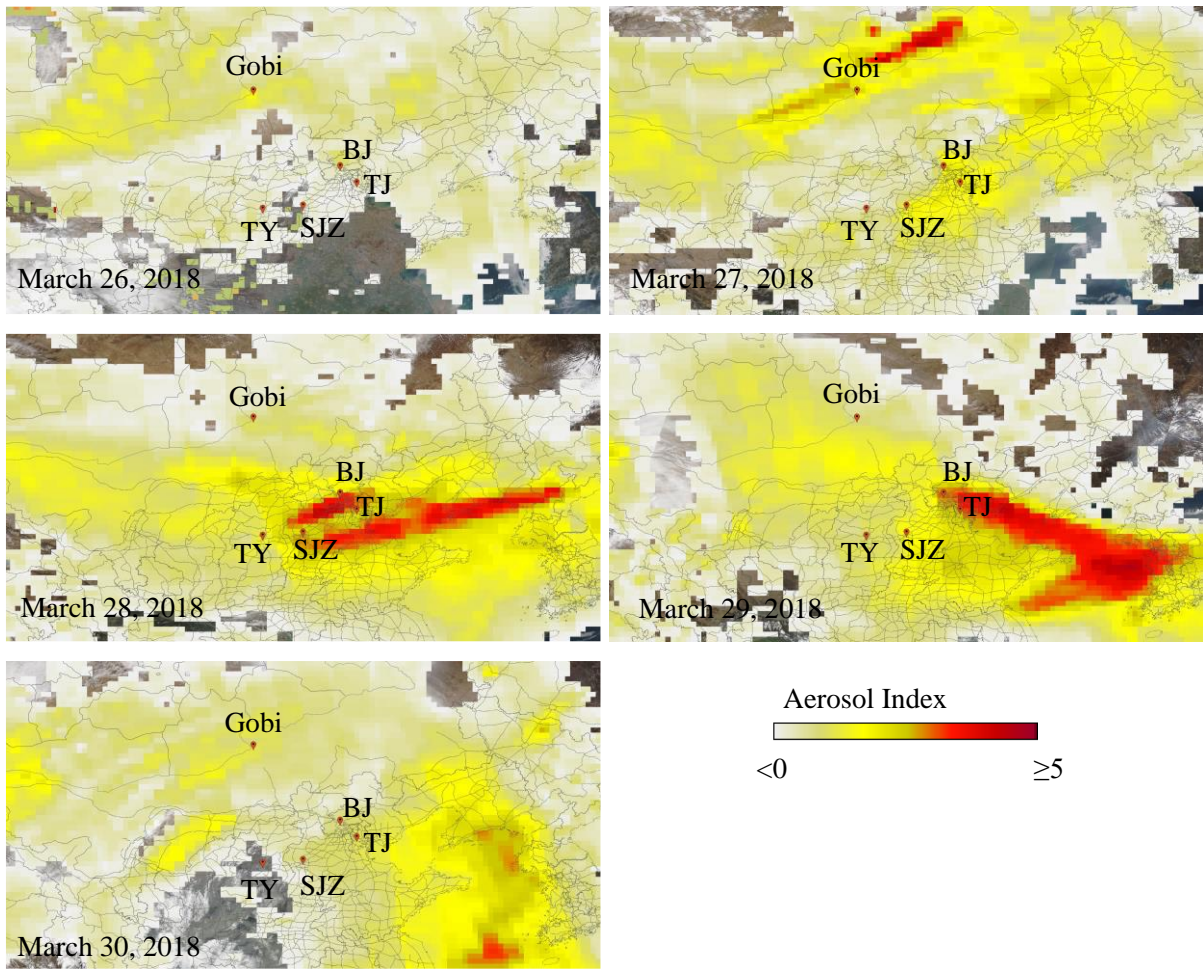


Figure S2. MODIS satellite image over North China Plain during the sampling period obtained from NASA (<https://worldview.earthdata.nasa.gov/>, last access on 7 Feb 2025). Red dots represent four sampling sites in the North China Plain.

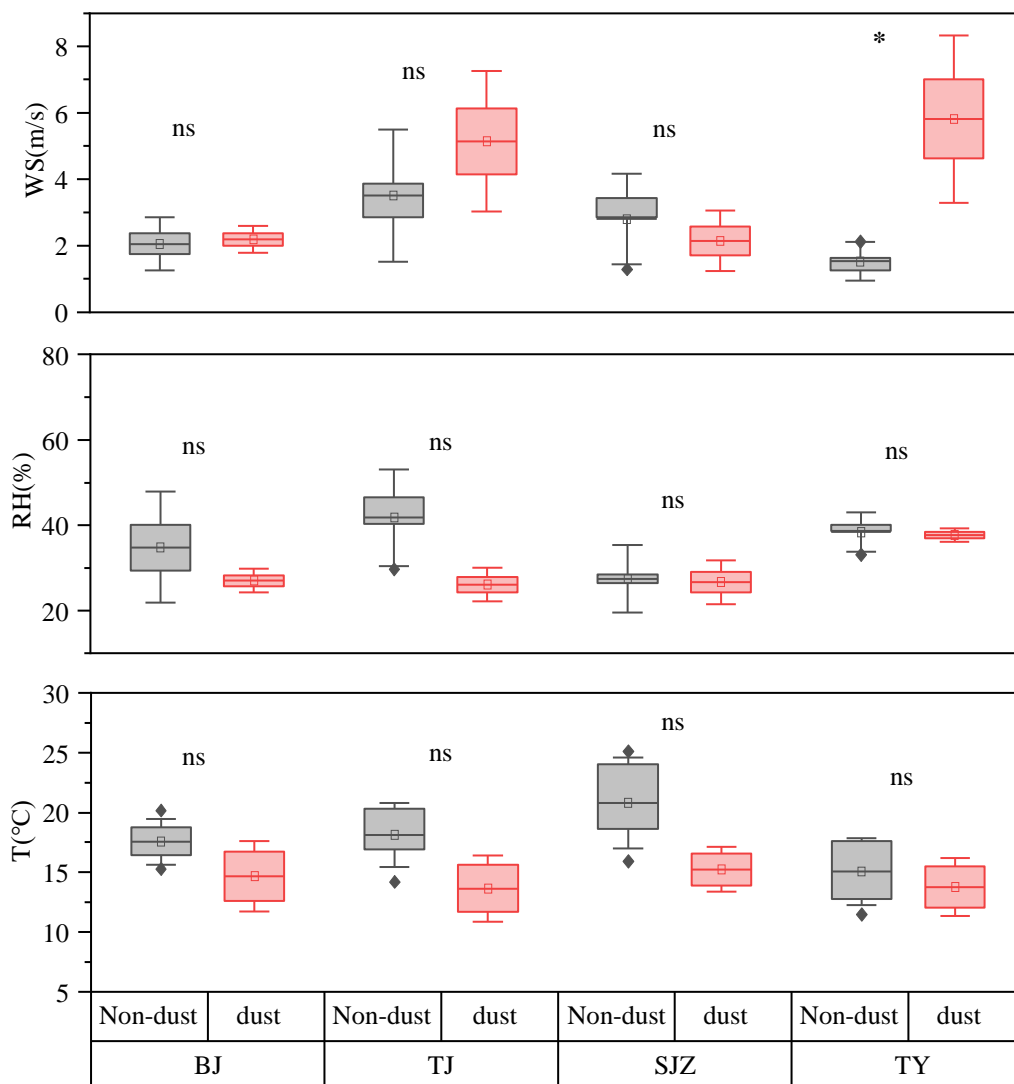


Figure S3. Comparison of meteorological parameters (wind speed-WS, relative humidity-RH and temperature-T) between the non-dust and dust period. The box encompasses the 25th–75th percentiles, whiskers, and line in each box are the SD and mean values, respectively. The symbol of * indicates differences between the dust and non-dust period. n.s.: not significant. The significance level was set at $p < 0.05$.

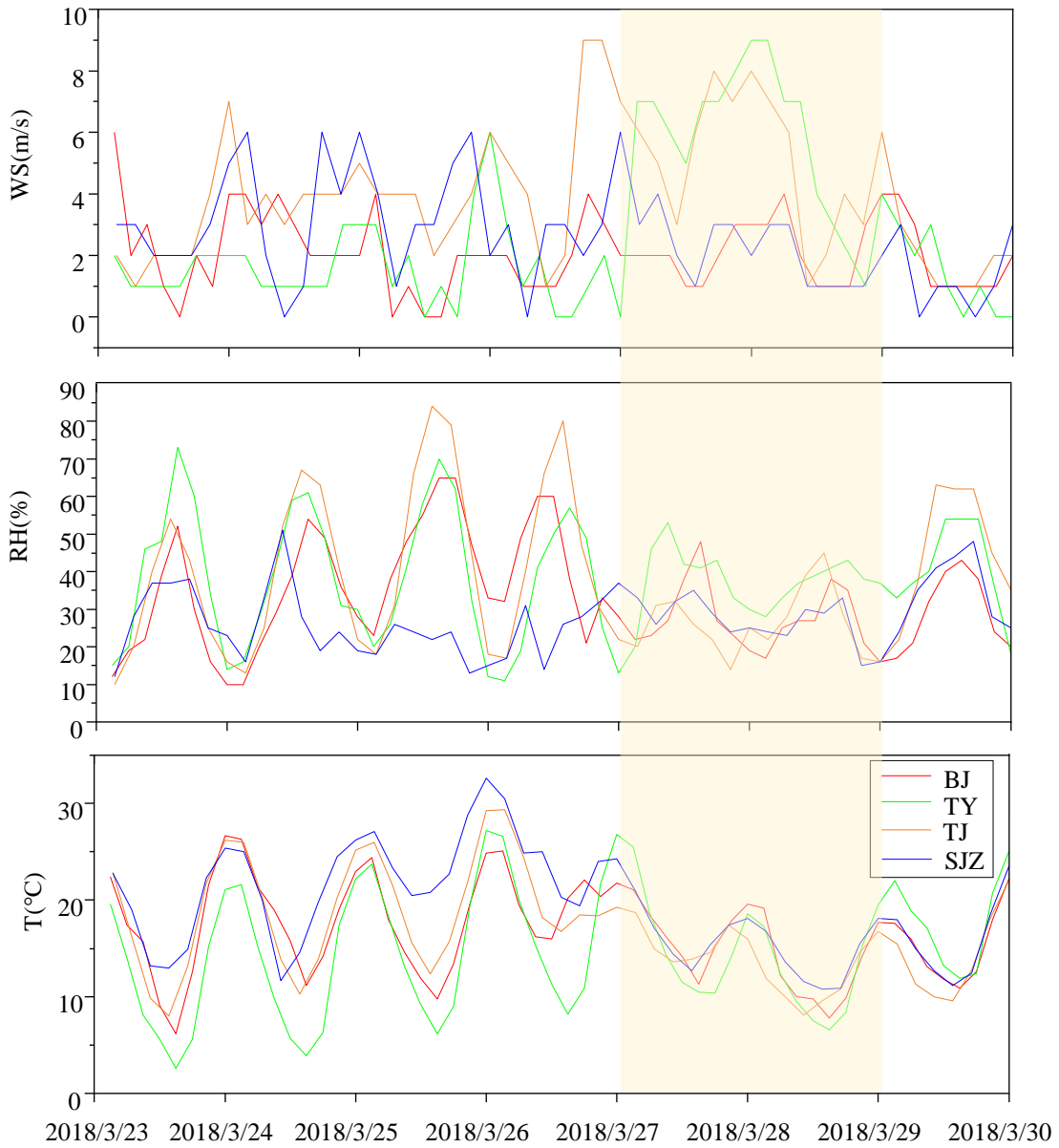


Figure S4. Meteorological parameters (wind speed-WS, relative humidity-RH and temperature-T) across the North China Plain during the sampling period. The yellow shaded area represents the dust period.

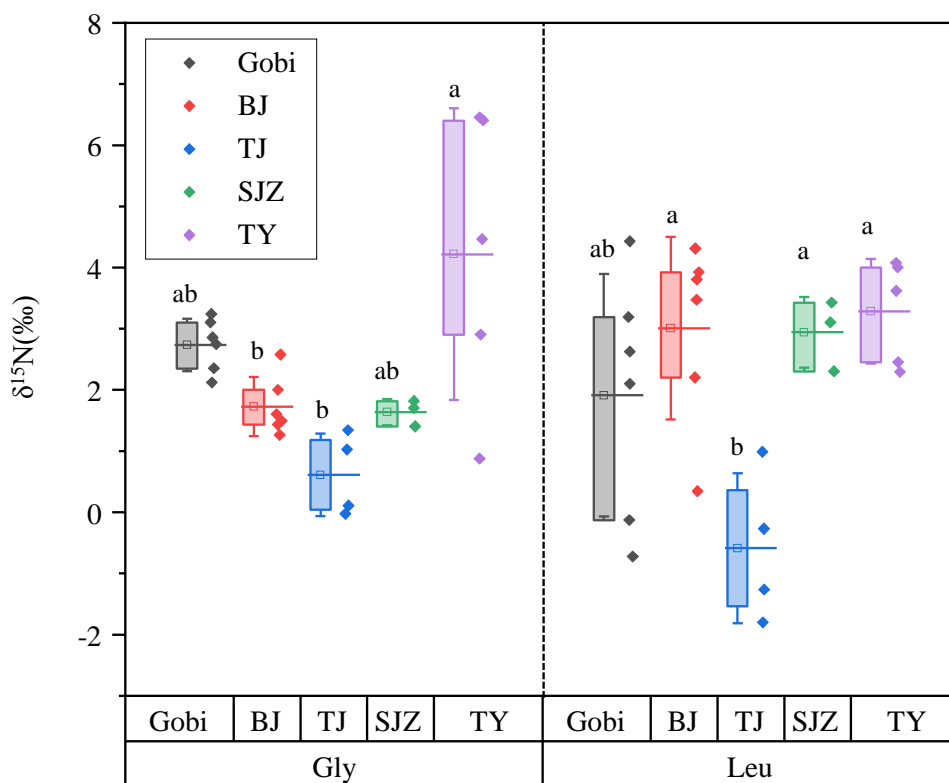


Figure S5. Box-and-whisker plots show the $\delta^{15}\text{N}$ values of combined Gly and Leu in the surface dust from the Gobi Desert and road dust from four North China Plain. Each box encompasses the 25th-75th percentiles. Whiskers and hollow squares inside each box are the SD and mean values, respectively. Dots are replicate measurements at each site. Differences in $\delta^{15}\text{N}$ values of combined Gly and combined Leu between the Gobi Desert and four North China Plain cities were examined using one-way ANOVA with Tukey's HSD test ($p < 0.05$). Statistically significant differences in mean Gly or Leu values between the Gobi Desert and individual cities are indicated by different letters (Tukey's HSD test).

References

- Stock, B. C. and B. X. Semmens. MixSIAR GUI User Manual. Version 3.1. <https://github.com/brianstock/MixSIAR/>. doi:10.5281/zenodo.47719. 2016.
- Song, W., Liu, X.-Y., Hu, C.-C., Chen, G.-Y., Liu, X.-J., Walters, W. W., Michalski, G., and Liu, C.-Q.: Important contributions of non-fossil fuel nitrogen oxides emissions, *Nat. Commun.*, 12, 243, <https://doi.org/10.1038/s41467-020-20356-0>, 2021.